

Electronic structure and magnetism in compressed 3d transition metals

Valentin Iota,^{a)} Jae-Hyun Park Klepeis, and Choong-Shik Yoo
Lawrence Livermore National Laboratory, Livermore, California 94550

Jonathan Lang, Daniel Haskel, and George Srajer
Advanced Photon Source, Argonne National Laboratory, Argonne, Illinois 60439

(Received 8 September 2006; accepted 21 December 2006; published online 24 January 2007)

The authors present a systematic study of high-pressure effects on electronic structure and magnetism in 3d transition metals (Fe, Co, and Ni) based on x-ray magnetic circular dichroism measurements. The data show that the net magnetic moment in Fe vanishes above 18 GPa upon the transition to hcp Fe, while both cobalt and nickel remain ferromagnetic to well over 100 GPa. The authors estimate the total disappearance of moment in hcp Co at around 150 GPa and predict a nonmagnetic Ni phase above 250 GPa. The present data suggest that the suppression of ferromagnetism in Fe, Co, and Ni is due to pressure-induced broadening of the 3d valence bands.

© 2007 American Institute of Physics. [DOI: 10.1063/1.2434184]

In ferromagnetic Fe, Co, and Ni, the partial filling of narrow 3d bands following Hund's rules and high electron density of states near the Fermi level result in a spin polarized valence band.¹ Magnetism, in turn, influences the structural properties of these electron-correlated metals, stabilizing bcc Fe and hcp Co (instead of the hcp Fe and fcc Co predicted without spin polarization).²⁻⁴

Under pressure, the steeper increase in electron kinetic energy versus potential energy diminishes the importance of Coulomb correlations.^{4,5} Accordingly, at sufficiently high pressures, Fe, Co, and Ni are all presumed uncorrelated metals.⁵ However, this has been established only in the case of iron,⁶⁻⁹ while virtually no magnetic measurements under pressure have been reported in Co or Ni.

In Fe, previous Mössbauer,⁶ K_{β} nonresonant emission,⁷ and x-ray magnetic circular dichroism⁸ (XMCD) spectroscopies show that the α (bcc)- to ϵ (hcp)-phase transition between 12 and 18 GPa (Ref. 9) is accompanied by the disappearance of the magnetic moments, suggesting that the hcp phase is nonmagnetic. Mathon *et al.* report K -edge XMCD measurements of Fe up to 23 GPa, showing that the magnetic transition precedes the structural bcc-hcp transition in Fe.⁸ In Co and Ni the magnetism dependence on volume has been derived only indirectly, from measurements of structural and elastic properties. A pressure-induced suppression of magnetic correlations is predicted to accompany the Co hcp-fcc transition (105–150 GPa).¹⁰⁻¹² No structural transitions have been reported in fcc Ni to above 100 GPa,¹³ and density functional theory (DFT) calculations show fcc Ni to be stable up to 34 TPa.⁵ Calculations predict slowly diminishing magnetic moments in fcc Ni up to 300 GPa, with vanishing moments in bcc Ni for volumes below 0.62 a.u.^{3,14}

Here, we report x-ray absorption near-edge spectroscopy (XANES) and XMCD measurements at the K edges of all three ferromagnetic 3d transition metals (Fe, Co, and Ni) for pressures up to 100 GPa.

High purity iron, cobalt, and nickel samples (99.9% purity, 5 μm foil) were loaded in diamond-anvil cells using mineral oil as pressure medium. To minimize diamond x-ray absorption, we employed perforated diamond-backing plates in conjunction with miniature anvils. Pressures were mea-

sured by ruby fluorescence method. Measurements were conducted at ambient temperature (293 K).

XANES and XMCD spectra were measured in transmission geometry at beamline 4ID-D at the Advanced Photon Source. The incident monochromatic radiation with an energy resolution $\Delta E=1$ eV was circularly polarized ($P_c = \pm 0.98$) and focused to a $\sim 10 \times 10 \mu\text{m}^2$ spot. A polarizing field of approximately 3 kOe along the x-ray direction was applied using high-field toroidal NdFeB permanent magnets positioned around the diamonds. In each run, the XMCD signal at low pressure was consistent with magnetizations approaching full saturation (within 3%–8% from the standard XMCD for each sample).

The K -edge XMCD data for all three metals have been reported at ambient pressure and the XMCD signal has been shown to scale with the 4p conduction band spin polarization.^{16,17} Changes in the 3d moment affect the exchange splitting of the 4p band, and hence the XMCD. Thus, the K -edge XMCD signal can be used as a measure of the magnetic moment under pressure.^{8,17}

Figure 1 summarizes the pressure-induced changes in the K -edge XMCD in Fe, Co, and Ni. The spectra are normalized to the edge jump and are shifted so as to align the Fermi respective levels for Fe (7112 eV), Co (7709 eV), and Ni (8333 eV). The XMCD signal decreases with pressure in all three metals. However, while in Fe the XMCD is virtually null by 23 GPa, in cobalt and nickel, the dichroism remains measurable up to 100 and 70 GPa, respectively (maximum pressures reached).

Figure 2 illustrates the XMCD versus compression factor (V/V_0) for each metal. In Fe, the XMCD signal decreases slightly but measurably in the bcc phase (up to 12 GPa), then declines sharply across the bcc-hcp transition (12–16 GPa), and virtually disappears in the hcp phase (23 GPa). At this pressure, x-ray diffraction confirmed a complete transformation to hcp Fe. Since the K -edge XMCD is proportional to the spin polarization of p -projected density of states near the Fermi level,¹⁵ the lack of XMCD in hcp Fe suggests a loss of spin polarization in the 4p conduction states above the Fermi level. Since spin fluctuations in conduction bands are responsible for long-range coupling of magnetic moments, the rapid decrease of dichroism across the bcc-hcp transition indicates a loss of long-range ferromagnetic order in hcp Fe. This

^{a)}Electronic mail: iota1@llnl.gov

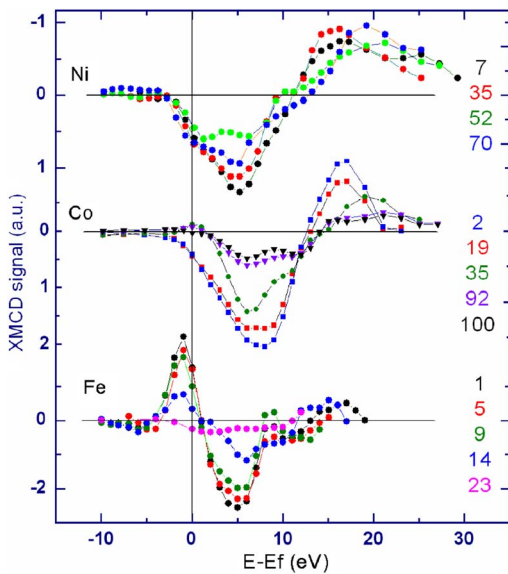


FIG. 1. (Color online) XMCD spectra for iron, cobalt, and nickel as a function of pressure. The energy scale is relative to the K -edge energy: 7112 eV for Fe, 7709 eV for Co, and 8333 eV for Ni. All spectra are normalized to the amplitude of the edge jump.

result is consistent with previous magnetic measurements in hexagonal iron under pressure.^{6–8,18}

In cobalt, the decrease in dichroism with pressure is uniform, suggesting a gradual decline in magnetic moment over the entire hcp-Co domain of stability. Our data show no first-order magnetic transition in cobalt up to 100 GPa. At this pressure, hcp Co remains weakly ferromagnetic with a magnetic moment of $\sim 0.3\mu_B$ (Fig. 2). This decrease of the magnetic moment in hcp Co with compression is not incompatible with the increase in the Curie temperature suggested from previous phase-structural considerations.¹⁰ The two properties need not be correlated (e.g., in the case of Fe and Co, with Curie points of 1043 and 1388 K, and ambient magnetic moments of $2.2\mu_B$ and $1.7\mu_B$, respectively).

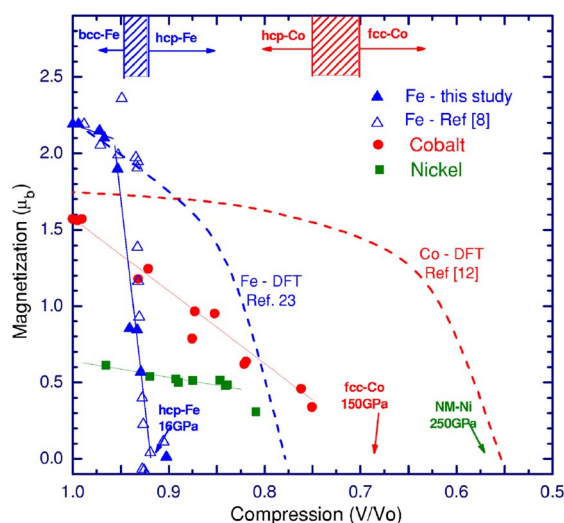


FIG. 2. (Color online) Net magnetic moment for iron, cobalt, and nickel as a function of compression. The data points represent measured XMCD signal scaled to the standard moment for each material (Fe: $2.2\mu_B$, Co: $1.6\mu_B$, and Ni: $0.6\mu_B$). The solid lines represent linear fits of the data, extrapolated to reach the x axis (vanishing moments). The dotted lines represent the results of DFT calculations for hcp phase of iron (in blue) and cobalt (in red) (Ref. 12).

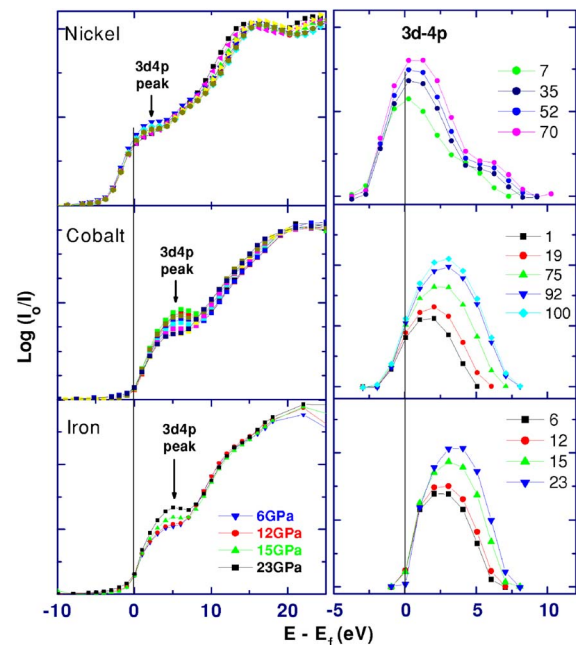


FIG. 3. (Color online) XANES spectra in Fe, Co, and Ni with pressure. On the right is a detail of the near-edge peak associated with transitions into mixed $3d-4p$ final states. The increase with pressure of the edge peak suggests increased delocalization of $3d$ electrons (band broadening).

The XMCD data show a much steeper decline in magnetic moment with pressure than that predicted by DFT calculations theory (dotted red line in Fig. 2).¹² Our XMCD data suggest that the magnetic moment in hcp cobalt would completely vanish before a compression of $\sim 0.7V_0$, corresponding to a pressure of ~ 150 GPa, slightly lower than the 180 GPa value predicted from DFT calculations. Since the hcp-fcc transformation in cobalt occurs between 105 and 150 GPa, the disappearance of magnetic moment occurs within the stability domain of fcc Co. This result would be consistent with a nonmagnetic fcc Co, as proposed earlier from structural and theoretical considerations.^{10–12}

In nickel, the magnitude of the moment at ambient conditions is smaller ($0.6\mu_B$), resulting in a weaker ferromagnetic coupling. As in bcc Fe and Co, the dichroism decreases uniformly with compression, but that the rate of decrease ($2.5 \times 10^{-3}\mu_B/\text{GPa}$) is smaller than in either Fe or Co. The smaller effect of volume on the magnetism in Ni is not unexpected, considering the smaller contribution of magnetism to the structural properties of Ni compared to Fe and Co.^{3,4,12}

The XMCD results summarized in Fig. 2 suggest that the rate of pressure-induced extinction of magnetism correlates inversely with the magnitude of the initial moment. That is, the material with the highest ambient pressure moment (Fe, $2.2\mu_B$) undergoes magnetic extinction at the lowest pressure (~ 12 – 18 GPa), while nickel, the weakest ferromagnet of the series ($0.6\mu_B$ initial moment), is the last to become nonmagnetic, well above 200 GPa. Furthermore, we find that in the absence of structural phase transitions, the magnetic moment decreases uniformly with pressure. This is in contrast to the previous theoretical calculations¹¹ suggesting that the magnetic moment of hcp Co remains nearly constant below 100 GPa (see Fig. 2).

To understand this result, we measured the near- K -edge x-ray absorption spectra for each of the three metals studied (Fig. 3). The relative intensity of the XANES peak (shown in

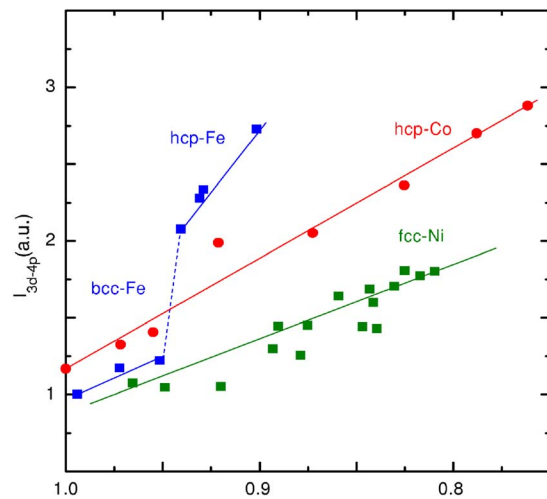


FIG. 4. (Color online) Intensity of the $3d-4p$ spectral feature as a function of compression showing increased $3d-4p$ hybridization (Ref. 19). The discontinuous jump observed in the Fe corresponds to a transition to a higher coordinated hcp structure above 12 GPa.

detail in Fig. 3, right panel) is a measure of the $3d-4p$ band hybridization in $3d$ transition metals.¹⁹

We observe significant increases in relative intensity and bandwidth of the preedge peak with pressure [shown in detail in Fig. 3(b)]. This suggests enhanced $3d-4p$ band overlaps (increased $3d$ bandwidth), resulting in diminished $3d$ electron correlations and a reduction in magnetic moment.

The Stoner criterion for an itinerant ferromagnet is given by $N(\epsilon_F)I > 1$.²⁰ Here, $N(\epsilon_F)$ represents the density of states (DOS) at the Fermi level, and I is the Stoner parameter (exchange integral), measuring the strength of exchange interaction and is sensitive to the localization of the wave functions at the Fermi level.²¹ In a first approximation, the Stoner parameter I is independent of volume, and the response of magnetization to pressure is fully contained in the density of states at the Fermi level $N(\epsilon_F)$.

Then, the observed increase in $3d$ bandwidth with pressure lowers the $3d$ DOS at the Fermi level, reducing the corresponding term in the Stoner equation and weakening the condition for ferromagnetism. This is consistent with *ab initio* calculations in bcc Fe showing a 40% decrease in $\text{DOS}(E_F)$ corresponding to a volume reduction from 70 to 50 a.u.³²² Our results support the conclusions that pressure enhances the overlap of the atomic wave functions, broadening the d bands close to E_F and lowering the $\text{DOS}(E_F)$.

In Co and Ni the observed decrease is gradual, since no structural transformations occur in the pressure range studied. Iron, however, undergoes its martensitic transformation between 12 and 18 GPa, from a magnetic bcc to a nonmagnetic hcp structure. In this case, in addition to the pressure-induced electron delocalization observed in the bcc phase, the $3d$ bandwidth W_{3d} increases discontinuously due to the jump in atomic coordination from 8 in bcc Fe to 12 in hcp Fe (Fig. 4). Across the bcc-hcp transition (12–18 GPa) pressure affects the magnetic moment via two separate mechanisms with converging effects. Increased pressure (i) diminishes the proportion of magnetic bcc component in the mixed phase and (ii) suppresses the net moment in the residual bcc phase via $3d$ band broadening. This may help explain why the net magnetic moment does not scale linearly with the bcc/hcp ratio in the phase transition region, as reported in Ref. 8. A

similar but substantially smaller effect can be expected to take place in cobalt between 105 and 150 GPa where both hcp and fcc phases coexist, as both the residual hcp proportion and the net moment in hcp Co are reduced by pressure. In contrast, in Ni, no structural transitions are expected, and we predict a gradual, second-order transition to a nonmagnetic fcc-Ni phase above 250 GPa.

In summary, we have described the pressure-induced electronic and magnetic changes in elemental iron, cobalt, and nickel to 23, 100, and 70 GPa, respectively. While iron shows a rather abrupt magnetic disappearance across the bcc-hcp phase boundary, Co and Ni gradually lose their magnetic moments but remain ferromagnetic over the entire pressure range studied. The extrapolation of the present data suggests the onset of nonmagnetic Co at around 150 GPa (within the pressure range of the previously reported structural phase transition) and a new nonmagnetic phase of Ni above 250 GPa. The suppression of long-range magnetic order in all three materials correlates well with the pressure-induced enhancement in $3d-4p$ hybridization ($3d$ band broadening), which contributes to a lower density of states at the Fermi level, N_F .

The work at LLNL was performed under the auspices of the U.S. DOE University of California, under Contract No. W-7405-Eng-48. The work at the APS was supported by the U.S. DOE, Office of Science, Contract No. DE-AC02-06CH11357.

¹G. A. Landrum and R. Dronskowski, *Angew. Chem., Int. Ed.* **39**, 1560 (2000).

²D. A. Young, *Phase Diagrams of the Elements* (University of California Press, Berkeley, 1991), pp. 177-182.

³H. Hasegawa and D. Pettifor, *Phys. Rev. Lett.* **50**, 130 (1983); H. L. Skriver, *Phys. Rev. B* **31**, 1909 (1985).

⁴P. Söderlind, R. Ahuja, O. Eriksson, J. M. Wills, and B. Johansson, *Phys. Rev. B* **50**, 5918 (1994).

⁵A. K. McMahon and R. C. Alberts, *Phys. Rev. Lett.* **49**, 1198 (1982).

⁶G. Cort, R. D. Taylor, and J. O. Willis, *J. Appl. Phys.* **53**, 2064 (1982).

⁷J. P. Rueff, M. Krisch, Y. Q. Cai, A. Kaprolat, M. Hanfland, M. Lorenzen, C. Masciovecchio, R. Verbeni, and F. Sette, *Phys. Rev. B* **60**, 14510 (1999).

⁸O. Mathon, F. Baudelet, J. P. Itié, A. Polian, M. D'Astuto, J. C. Chervin, and S. Pascarelli, *Phys. Rev. Lett.* **93**, 255503 (2004).

⁹N. von Bargen and R. Boehler, *High Press. Res.* **6**, 133 (1990).

¹⁰C. S. Yoo, H. Cynn, P. Söderlind, and V. Iota, *Phys. Rev. Lett.* **84**, 4132 (2000).

¹¹A. F. Goncharov, J. Crowhurst, and J. M. Zaug, *Phys. Rev. Lett.* **92**, 115502 (2004).

¹²G. Steinle-Neumann, L. Stixrude, and R. E. Cohen, *Phys. Rev. B* **60**, 791 (1999).

¹³P. Lazor and S. K. Saxena, *Terra Abstr.* **5**, 363 (1993).

¹⁴T. Jarlborg, *Physica C* **385**, 513 (2003); M. Uhl and J. Kübler, *Phys. Rev. Lett.* **77**, 334 (1996).

¹⁵A. Dadashev, M. P. Pasternak, G. Kh. Rozenberg, and R. D. Taylor, *Rev. Sci. Instrum.* **72**, 2633 (2001).

¹⁶G. Schütz, W. Wagner, W. Wilhelm, and P. Kienle, *Phys. Rev. Lett.* **58**, 737 (1987); S. Stahler, G. Schutz, and H. Ebert, *Phys. Rev. B* **47**, 818 (1993).

¹⁷F. Baudelet, S. Pascarelli, O. Mathon, J. P. Itié, A. Polian, M. d'Astuto, and J. C. Chervin, *J. Phys.: Condens. Matter* **17**, S957 (2005).

¹⁸R. D. Taylor, M. P. Pasternak, and R. Jeanloz, *J. Appl. Phys.* **69**, 6126 (1991).

¹⁹T. E. Westre, P. Kennepohl, J. G. DeWitt, B. Hedman, K. O. Hodgson, and E. I. Solomon, *J. Am. Chem. Soc.* **119**, 6297 (1997).

²⁰E. C. Stoner, *Proc. R. Soc. London, Ser. A* **165**, 372 (1938).

²¹D. M. Edwards and E. P. Wohlfarth, *Proc. R. Soc. London, Ser. A* **303**, 127 (1968).

²²M. Ekman, B. Sadigh, K. Einarsson, and P. Blaha, *Phys. Rev. B* **58**, 5296 (1998).